

RESEARCH ON RAILWAY TRACK EDGE DETECTION BASED ON BM3D AND ZERNIKE MOMENTS

Nan WANG¹, Tao HOU², Tianming ZHANG³

^{1,2,3} School of Automation and Electrical Engineering, Lanzhou Jiaotong University, Lanzhou, China

Abstract:

With the rapid development of intelligent rail transportation, the realization of intelligent detection of railroad foreign body intrusion has become an important topic of current research. Accurate detection of rail edge location, and then delineate the danger area is the premise and basis for railroad track foreign object intrusion detection. The application of a single edge detection algorithm in the process of rail identification is likely to cause the problem of missing important edges and weak gradient change edges of railroad tracks. It will affect the subsequent detection of track foreign objects. A combined global and local edge detection method is proposed to detect the edges of railroad tracks. In the global pixel-level edge detection, an improved blok-matching and 3D filtering (BM3D) algorithm combined with bilateral filtering is used for denoising to eliminate the interference information in the complex environment. Then the gradient direction is added to the Canny operator, the computational template is increased to achieve non-extreme value suppression, and the Otsu thresholding segmentation algorithm is used for thresholding improvement. It can effectively suppress noise while preserving image details, and improve the accuracy and efficiency of detection at the pixel level. For local subpixel-level edge detection, the improved Zernike moment algorithm is used to extract the edges of the obtained pixel-level images and obtain the corresponding subpixel-level images. It can enhance the extraction of tiny feature edges, effectively reduce the computational effort and obtain the subpixel edges of the orbit images. The experimental results show that compared with other improved algorithms, the method proposed in this paper can effectively extract the track edges of the detected images with higher accuracy, better preserve the track edge features, reduce the appearance of pseudo-edges, and shorten the edge detection time with certain noise immunity, which provides a reliable basis for subsequent track detection and analysis.

Keywords: rail track, edge detection, BM3D, Zernike moments, Canny operator

To cite this article:

Wang, N., Hou, T., Zhang, T., (2023). Research on railway track edge detection based on BM3D and Zernike moments. *Archives of Transport*, 68(4), 7-20. DOI: <https://doi.org/10.61089/aot2023.fz9g6c16>



Contact:

1) 11210404@stu.lzjtu.edu.cn [<http://orcid.org/0009-0006-7952-6989>] – corresponding author; 2) ht_houtao@163.com [<http://orcid.org/0000-0002-7511-3013>]; 3) 1220014639@qq.com [<http://orcid.org/0009-0009-3731-7566>]

1. Introduction

With the rapid development of intelligent rail transportation, achieving intelligent detection of foreign object incursions on railways has become an important research topic. The proportion of high-speed rail vehicles among the rolling stock providing public transportation services is increasing (Krzysztof et al., 2022). Railroad safety is very important, so while building intelligent railroads, higher requirements are placed on train safety (Karolak, 2021). And railroad safety technology should be strengthened (Burdzik et al., 2017). Accurate detection of rail positions is a prerequisite and foundation for determining areas of rail encroachment, and the results of track edge detection determine the scope of foreign object detection on railways. It is necessary to divide a dangerous area based on the track, and merely detects the foreign object in the dangerous area (Niu et al., 2018). Due to the long-term exposure of steel rails to outdoor environments, complex surroundings, and issues such as rail aging, the accuracy and robustness of rail edge detection are affected.

In order to improve the accuracy of railway track edge detection, especially in cases where the distant ends are heavily influenced by factors such as lighting and environmental noise, this paper proposes a sub-pixel edge detection method. Sub-pixel edge detection aims to enhance the accuracy of edge detection through software algorithms while maintaining hardware conditions, thus improving the quality of edge detection without increasing costs.

To address the limitations of existing Canny edge detection methods in terms of noise reduction and edge detection, this paper presents improvements to the Canny algorithm. Firstly, we enhance the Block-Matching and 3D Filtering (BM3D) algorithm (Goyal et al., 2020) and apply the improved BM3D algorithm to filter the images. Then, the improved Canny operator is used to extract edges from the filtered images. To enhance the resolution of the extracted images, an improved Zernike moment-based sub-pixel edge detection method is introduced. Sub-pixel detection enhances the detection quality of pixels from the edges to the interior, and the improved Zernike moment method is employed to detect sub-pixel positions of various edges in railway track images, thereby improving the accuracy of track edge extraction.

Through these improvements, this paper aims to enhance the accuracy and reliability of railway track edge detection, particularly in situations where interference is present. This sub-pixel edge detection method enables fine extraction of track edges while maintaining the same camera resolution.

Aiming at the challenge of railroad track image edge detection which easily causes the missing of important edges and weak gradient change edges of the railroad track, this paper proposes a railroad track edge detection method based on BM3D and Zernike moments. Firstly, the Canny algorithm is improved to address the shortcomings of the existing Canny edge detection algorithm in terms of noise removal and edge detection, and by combining the BM3D filtering algorithm and the Zernike moments subpixel edge detection algorithm, the effective extraction of pixel-level and subpixel-level edges is realized. Secondly, in order to further verify the performance of the improved algorithm, the proposed method is experimentally verified and compared with the general algorithm to demonstrate the superiority and feasibility of the improved algorithm in the edge detection of railroad tracks, and the experimental results show that the method has high edge detection accuracy and fast detection speed.

2. Literature review

Existing edge detection research primarily utilizes two approaches: classical methods and deep learning-based methods. Liu Huizhong et al. (2022) proposed an optimized Canny edge detection algorithm and the HED (holistically-nested edge detection) algorithm based on deep learning. The optimized HED algorithm can effectively identify the edge information of mining belts. Liu Yun et al. (2019) proposed an edge detection model based on RCF (richer convolutional feature), which employs more comprehensive convolutional features to enhance the performance of the edge detection model. These deep learning-based methods address edge detection challenges but suffer from issues such as high computational complexity, poor real-time performance, and high hardware requirements. Classical edge detection methods are based on grayscale variations at image edges, such as the Roberts, Prewitt, Sobel, and Canny operators (Fu et al., 2020). Among these, the Canny operator is widely used in railway track edge detection due to its excellent signal-to-noise ratio and detection accuracy. However, the Canny

edge detection method requires improvements due to factors like illumination and complex backgrounds. Luo Wenting et al. (2018) replaced Gaussian filtering with Wiener filtering and utilized the Otsu algorithm to adaptively select image thresholds, reducing noise and false edges. Archana P. et al. (2019) proposed combining the Canny operator with mathematical morphology to automatically select the threshold required for segmenting gradient images. However, their method exhibits lower detection efficiency and lacks real-time performance. Song Yafan et al. (2018) presented a complex environment railway track recognition method based on salient features, which is suitable for track recognition in complex environments. However, the directional nature of edge detection results in insufficient accuracy in track edge detection. Bojarczak et al. (2019) proposed to use wavelet transform in the precise positioning of railroad track edges. Gong S et al. (2019) introduced bilateral filtering for image denoising and adaptive threshold selection for edge detection. This algorithm exhibits prominent performance in the presence of noise, particularly for the distinct shape of sleepers.

Some mathematics-related methods are also often used for track detection. Zheng Yunshui et al. (2020) propose a convenient and fast image track identification method based on line segment detector (LSD) and least-squares curve fitting. Wang Zhongli et al. (2017) propose a geometric constraint-based track detection method that uses the relationship between the camera and the track plane to approximately satisfy the monophonic matrix feature of inverse perspective mapping for segmented track detection method. Soilan et al. (2021) applied a fully automated method for point cloud segmentation of point cloud data acquired by on-board radar to extract and depict the location and geometric structure of rail tracks, and roughly estimated and extracted rail track point cloud data. Zhang Yan (2022) proposed a point cloud data-based rail track identification method for point cloud data acquired by airborne LiDAR for rail track identification.

The implementation of rail identification can make rail survey, rail flaw detection and rail intrusion detection (Liu et al., 2020) and other technologies better, can reduce the number of staff to reach the rail location for field survey, can reduce labor and time costs, improve efficiency, but also can provide a better working environment for staff. Thus, an essential

key technology for railway foreign object incursion detection lies in effectively mitigating the influence of noise on edge detection while accurately detecting track edges.

3. Image filtering

The quality of image preprocessing is crucial for subsequent image processing tasks. It is important to remove irrelevant information from the signal while preserving the integrity of the original image. Filtering plays a significant role in achieving this goal. The BM3D algorithm, which combines block matching and three-dimensional transform domain filtering, is an effective denoising algorithm that can eliminate noise without affecting image edges. The BM3D algorithm consists of two main stages: basic estimation and final estimation, each comprising three steps. In the first step, similar blocks are matched for each reference block, forming a three-dimensional group. Collaborative filtering is then applied to the group in the second step. Finally, the filtering results of the corresponding groups for each reference block are aggregated to obtain the denoised result. However, in the case of railway track images captured in complex environments, the conventional BM3D algorithm may overlook certain image details and may not be suitable. Therefore, improvements have been made to address this limitation and enhance the performance of the BM3D algorithm for railway track images.

Basic Estimation Stage (Cui et al., 2021): The improved BM3D algorithm incorporates a wider search range for similar blocks in edge regions and employs soft thresholding instead of hard thresholding in smooth regions. By extending the search range for similar blocks in edge regions, higher-quality similar blocks, which are typically absent in other areas, can be obtained. The soft thresholding is defined as shown in the following formula:

$$SF = \begin{cases} \text{sign}(X)(|X| - \tau), & \text{if } |X| > \tau \\ 0, & \text{if } |X| \leq \tau \end{cases} \quad (1)$$

where X is the transform coefficient; τ is the threshold value. For soft thresholding, if the absolute value of the transform coefficient is greater than the threshold, the threshold is subtracted from the transform coefficient; conversely, if the absolute value of the transform coefficient is less than or equal to the threshold, the transform coefficient is zero.

Final Estimation Stage: the conventional BM3D algorithm employs a Wiener filter optimized based on mean square error (MSE). MSE is an image quality evaluation metric that relies on pixel-wise errors and overlooks local information in non-smooth regions. To address the limitations of MSE, an improved approach is introduced using a Wiener filter optimized based on structural similarity (SSIM). SSIM is a novel image quality evaluation metric, which is defined as follows:

$$\text{SSIM}(x, y) = \frac{(2u_x u_y + c_1)(2\sigma_{xy} + c_2)}{(u_x^2 + u_y^2 + c_1)(\sigma_x^2 + \sigma_y^2 + c_2)} \quad (2)$$

where x and y denote two blocks at the same position in the image before and after denoising; u_x and u_y denote the average pixel values of x and y , respectively; σ_{xy} is the covariance of x and y pixel values; σ_x^2 and σ_y^2 denote the variance of x and y pixel values, respectively; c_1 and c_2 can be obtained from the equations $c_1 = (k_1 L)^2$, $c_2 = (k_2 L)^2$, and L is the dynamic range of pixel values.

For edge detection in railway track images, employing soft thresholding segmentation in the edge regions can yield clearer edge information while preserving important image features. Utilizing a Wiener filter optimized by SSIM for denoising can achieve better denoising results while preserving details. However, the BM3D algorithm may exhibit edge ringing artifacts when processing images with high contrast edges. Bilateral filtering can effectively achieve edge-preserving denoising. To obtain high-quality railway track images, this study combines bilateral filtering with the improved BM3D algorithm for image filtering.

Bilateral filtering (Lv et al., 2022) is a nonlinear spatial filtering technique that can effectively preserve edges while achieving noise reduction and smoothing. The output pixel value G of the noisy image after bilateral filtering is expressed as follows:

$$G(a, b) = \frac{\sum_{m,n} f(m, n) w(a, b, m, n)}{\sum_{m,n} w(a, b, m, n)} \quad (3)$$

where a, b denote the position of the central pixel point; m, n denote the position of the domain pixel, f is the noisy image, $f(m, n)$ is the gray value of the neighboring pixel point (m, n) ; the weight coefficient $w(a, b, m, n)$ is the product of the spatial domain kernel d and the value domain kernel r .

The spatial domain kernel d is based on a Gaussian function to calculate the Euclidean distance between the current point and the centroid, defined as follows:

$$d(a, b, m, n) = \exp\left(-\frac{(a-m)^2 + (b-n)^2}{2\sigma_d^2}\right) \quad (4)$$

where σ_d is the spatial domain standard deviation. The range kernel r is computed based on the absolute difference between the pixel values of the current point and the central point using a Gaussian function, defined as follows:

$$r(a, b, m, n) = \exp\left(-\frac{\|f(a,b) - f(m,n)\|^2}{2\sigma_r^2}\right) \quad (5)$$

where σ_r is the value domain standard deviation, $f(a, b)$ is the gray value of the center pixel point (a, b) . The calculation formula for the weighting coefficients can be derived from the formulas of the spatial domain kernel and the range domain kernel, as shown in the following equation:

$$w(a, b, m, n) = \exp\left(-\frac{(a-m)^2 + (b-n)^2}{2\sigma_d^2} - \frac{\|f(a,b) - f(m,n)\|^2}{2\sigma_r^2}\right) \quad (6)$$

The proposed algorithm begins by applying bilateral filtering to the noisy railway track image. Bilateral filtering is selected for its ability to preserve edges effectively, ensuring that the image retains well-defined edges. Despite this edge preservation, some Gaussian noise may still persist in the filtered image. To address this, an improved version of the BM3D algorithm is employed to further process the image. The detailed processing steps are illustrated in Fig.1.

4. Edge detection of railway tracks

4.1. Improved Canny algorithm

Improvements to the Canny algorithm have been made to overcome its weaknesses in noise resistance, potential blurring of image edges, limited ability to compute pixel gradients, inflexible threshold selection, and the risk of losing edge information. To address these issues, several enhancements have been implemented. Firstly, a combination of bilateral filtering and an improved BM3D algorithm is utilized as an alternative to the Gaussian filter for image filtering. This approach effectively preserves edge information while reducing Gaussian noise.

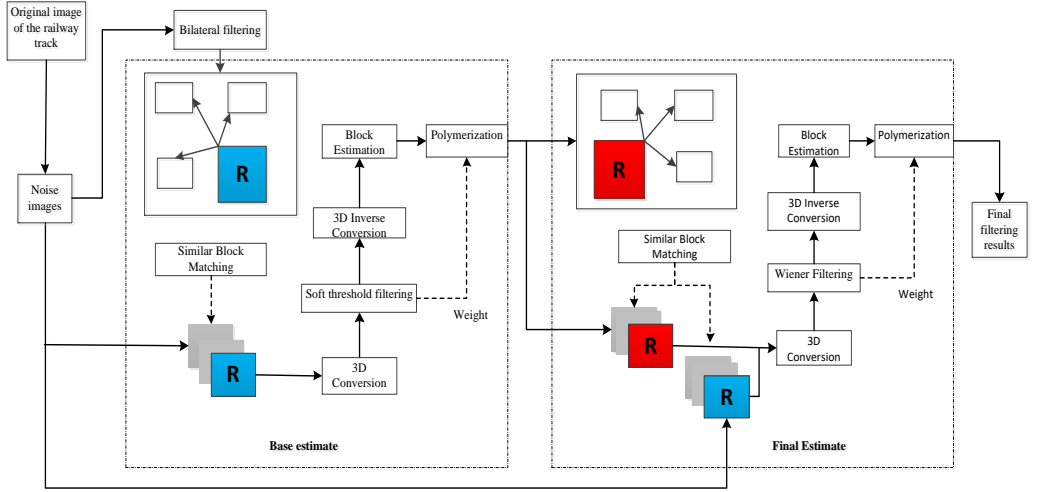


Fig. 1. Filtering algorithm processing process diagram

Secondly, to better adapt to the variations in images, additional gradient directions are incorporated into the traditional Sobel operator. By considering multiple gradient directions along with their magnitudes, the edge localization is enhanced through non-maximum suppression (Ren et al., 2018). Lastly, the Otsu thresholding algorithm is employed to determine dual thresholds for image thresholding. This adaptive thresholding method ensures optimal separation between background and foreground, resulting in improved edge detection. Overall, these enhancements result in an optimized Canny algorithm that addresses the limitations of the original approach, providing better noise reduction, edge preservation, and more accurate edge detection.

4.1.1. Improvement in Gradient Magnitude Calculation Method

The conventional Canny operator uses a 2×2 template to compute image gradients only in the horizontal and vertical directions, which fails to suppress noise effectively and can decrease edge localization accuracy (Sheshathri et al., 2019), resulting in more false edges and potential loss of true edges. To accommodate the arbitrary nature of captured railway track images, the improved gradient calculation incorporates multiple directional gradients. The enhanced gradient calculation, based on the traditional Sobel operator in horizontal and vertical directions,

also includes directions at 45° and 135° . Additionally, the 2×2 neighborhood is expanded to a 3×3 neighborhood, enhancing the image's anti-interference capability. Referring to Zhang Jiuchao et al. (2022), Eqs. 7-9 can be obtained. Then the image direction gradient is calculated as follows:

$$\begin{cases} G_x(m, n) = S(m+1, n) - S(m-1, n) \\ G_y(m, n) = S(m, n+1) - S(m, n-1) \\ G_{45^\circ}(m, n) = S(m+1, n+1) - S(m-1, n-1) \\ G_{135^\circ}(m, n) = S(m-1, n+1) - S(m+1, n-1) \end{cases} \quad (7)$$

where $S(m, n)$ denotes the image after convolution of the original image; $G(m, n)$ denotes the gradient in the direction of this image. Then the gradient amplitude is shown in the following equation:

$$M(m, n) = \frac{1}{\sqrt{G_x(m, n)^2 + G_y(m, n)^2 + G_{45^\circ}(m, n)^2 + G_{135^\circ}(m, n)^2}} \quad (8)$$

The formula for calculating the gradient direction in each direction is expressed as follows:

$$\theta(x, y) = \arctan\left(\frac{G_y(m, n)}{G_x(m, n)}\right) \quad (9)$$

4.1.2. Otsu thresholding algorithm

The Otsu thresholding algorithm (Rosnelly et al., 2020; Wei et al., 2019; Zheng et al., 2022) is a commonly used adaptive thresholding method that can

enhance the robustness of the algorithm when applied in edge detection. It provides a simple calculation and is less affected by variations in image brightness.

Let L denote the number of gray levels in the image, and n_i denote the number of pixels with gray level i . The histogram distribution of the image is illustrated as follows:

$$p_i = n_i/N, \sum_{i=0}^{L-1} p_i = 1 \quad (10)$$

Let S be the threshold value, and the gray levels can be divided into two classes: $C_0 = (0, 1, \dots, S)$ and $C_1 = (S+1, S+2, \dots, L-1)$. The average probabilities of the C_0 and C_1 classes can be represented as follows:

$$\begin{cases} w_0 = P_r(C_0) = \sum_{i=0}^{S-1} p_i \\ w_1 = P_r(C_1) = \sum_{i=S}^{L-1} p_i = 1 - w_0 \end{cases} \quad (11)$$

Then, the average grayscale values of regions C_0 and C_1 can be expressed as:

$$\begin{cases} u_0 = \sum_{i=0}^{S-1} iP_r(i|C_0) = \sum_{i=0}^{S-1} ip_i/w_0 = u(S)/w_0 \\ u_1 = \sum_{i=S}^{L-1} iP_r(i|C_1) = \sum_{i=S}^{L-1} ip_i/w_1 = \frac{u-u(S)}{1-w_0} \end{cases} \quad (12)$$

where u is the average gray level of the entire image, which can be calculated as:

$$u_T = \sum_{i=0}^{L-1} ip_i = P_0u_0 + P_1u_1 \quad (13)$$

The variance of C_0 and C_1 can be found by the following equation:

$$\begin{cases} \sigma_0^2 = \sum_{i=0}^S (i - u_0)^2 p_i/w_0 \\ \sigma_1^2 = \sum_{i=S+1}^{L-1} (i - u_1)^2 p_i/w_1 \end{cases} \quad (14)$$

So the total variance of the two regions is shown in the following equation:

$$\begin{aligned} \sigma_B^2 &= P_0(u_T - u_0)^2 + \\ &P_1(u_T - u_1)^2 = P_0P_1(u_0 - u_1)^2 \end{aligned} \quad (15)$$

Summarize above, the process of improving the Canny algorithm is as follows: Firstly, the original image is filtered using the proposed improved BM3D image filtering algorithm instead of a Gaussian filter. Next, the Sobel operator is used to compute the gradient direction and magnitude. Subsequently, non-maximum suppression is applied based

on the computed gradient direction and magnitude. Then, the Otsu thresholding algorithm is used to determine dual thresholds for image thresholding. Following the thresholding step, which uses the high and low thresholds, pixel-level edge localization is achieved.

4.2. Improved Zernike moments

This paper proposes an optimized sub-pixel edge detection method that improves the efficiency of edge detection while reducing computational complexity. The proposed approach combines the Canny algorithm for pixel-level edge detection with the Zernike moment sub-pixel edge detection algorithm (Liu et al., 2021).

In the sub-pixel edge detection stage, the image obtained from pixel-level edge detection is processed using the Zernike moment algorithm. This algorithm utilizes a predefined template and performs convolution between the image and the template to obtain Zernike moments. The rotational invariance property of the Zernike moment algorithm is leveraged to correct the moments and calculate four parameters: background gray value (h), vertical distance from the disc center to the edge (d), angle (φ) between the vertical line and the x-axis, and step height (k). These parameters enable the determination of whether a point is an edge and the calculation of the sub-pixel position of the edge point.

Importantly, the relationship between the Zernike moments before rotation (Z_{nm}) and after rotation (Z'_{nm}) can be expressed by a specific equation as follows:

$$Z'_{nm} = Z_{nm}e^{-nim\phi} \quad (16)$$

Let $f'(x, y)$ be the image after rotation, then we have:

$$\iint_{x^2+y^2 \leq 1} f'(x+y) y dx dy = 0 \quad (17)$$

The edge parameters are determined by the three Zernike moments Z_{00} , Z_{11} , and Z_{20} , and the corresponding complex numbers are $V_{00}=1$, $V_{11}=x+jy$ and $V_{20}=2x^2+2y^2-1$. Due to the rotational invariance, we have:

$$\begin{cases} Z'_{00} = Z_{00} \\ Z'_{11} = Z_{11}e^{j\phi} \\ Z'_{20} = Z_{20} \end{cases} \quad (18)$$

Further the Zernike moment of the image after rotation can be introduced as:

$$\left\{ \begin{aligned} Z'_{00} &= 2 \int_1^{-1} \int_0^{\sqrt{1-x^2}} h dy dx + 2 \int_1^1 \int_0^{\sqrt{1-x^2}} k dy dx \\ &= \dot{n}\pi + \frac{h\pi}{2} - k \sin^{-1}(l) - kl(\sqrt{1-l^2}) \\ Z'_{11} &= \iint_{x^2+y^2 \leq 1} f'(x, y)(x-yi) dy dx = \\ &\quad \frac{2k(1-l^2)^{3/2}}{3} \\ Z'_{20} &= \iint_{x^2+y^2 \leq 1} f'(x, y)(2x^3 + 2y^2 - 1) dy dx = \\ &\quad \frac{2kl(1-l^2)^{3/2}}{3} \end{aligned} \right. \quad (19)$$

Then finally, the four parameters of the ideal edge are derived as:

$$\left\{ \begin{aligned} h &= \frac{Z_{00} - \frac{k\pi}{2} + \pi \arcsin l + kl(\sqrt{1-l^2})}{\pi} \\ k &= \frac{3Z'_{11}}{2(1-l^2)^{3/2}} = \frac{3Z_{11}}{2(1-l^2)^{3/2}} e^{j\phi l} \\ \varphi_{nl} &= \tan^{-1} \left[\frac{\text{Im}[Z_{nl}]}{\text{Re}[Z_{nl}]} \right] (n = 1, 3) \\ l &= \frac{Z_{20}}{Z'_{11}} = \frac{Z_{20}}{Z_{11}} e^{-j\phi} \end{aligned} \right. \quad (20)$$

So, when using a template of size $N \times N$ to sample within the unit circle, the convolution operation between the template and its corresponding pixels yields the Zernike moment values of the image. The sub-pixel edge position in the Zernike moment-based sub-pixel edge detection method is determined as follows:

$$\begin{bmatrix} x' \\ y' \end{bmatrix} = \begin{bmatrix} x \\ y \end{bmatrix} + \frac{N}{2} \cdot l \begin{bmatrix} \cos \phi \\ \sin \phi \end{bmatrix} \quad (21)$$

In the Zernike moment algorithm, a fixed threshold is used. Ideally, the target pixels and non-target pixels are differentiated based on the threshold, maximizing the between-class variance of the target and non-target images (Ou et al., 2020). However, considering only the ideal edge model can result in blurry edges in the detected railway edges. Therefore, a method is proposed to calculate the edge parameters of each pixel near the railway edge using Zernike moments.

By setting a relative gray threshold q_1 and an intensity threshold q_2 , the algorithm searches for regions near the railway edge where the gray value is lower than the relative gray threshold q_1 . Along the gradient direction, points with intensity values greater

than the intensity threshold q_2 are identified. The set of pixel-level edge points is denoted as $\{P\}$, and based on Equation 21, the sub-pixel point set is obtained as follows:

$$\{P_e\} = \{(x_{1e}, y_{1e}), \dots, (x_{ie}, y_{ie}), \dots, (x_{ne}, y_{ne})\} \quad (22)$$

During the sub-pixel edge detection stage, the previously improved Canny operator is used to obtain a pixel-level edge detection image. The improved Zernike moments are then applied for sub-pixel edge detection. Compared to the previous detection method, there is no need to calculate multiple Zernike orthogonal complex moments for each pixel, which reduces the computational complexity during the edge detection process. Moreover, this approach enables the extraction of precise edge information. The detected railway edge information becomes clearer and more continuous, thereby enhancing the integrity of railway edge connections.

5. Experiment Results and Analysis

In order to validate the feasibility of the proposed algorithm, MATLAB 2018b software was used for simulation experiments to analyze the improved filtering algorithm and edge detection algorithm.

5.1. Experimental Results and Analysis of the Filtering Algorithm

To fully demonstrate the filtering performance of the proposed improved filtering algorithm, experiments were conducted to evaluate its ability to reduce noise in railway track images. Simulated noisy track images were generated by adding Gaussian noise with different standard deviations (σ) to clean track images. Then, the proposed filtering algorithm was applied to these noisy images to remove the noise. The experimental results are shown in Fig.2.

To quantitatively describe the denoising effect of the railway track images, this study employed peak signal-to-noise ratio (PSNR) and structural similarity index (SSIM) as quantitative analysis metrics for comparison. These metrics are shown in Fig. 3 and Fig. 4, respectively.

To visually demonstrate the effectiveness of the improved BM3D filtering algorithm, a 3D histogram was used as an experimental model, as shown in Fig.5. By comparing the denoised 3D histograms of the track images, it can be observed that mean filtering causes boundary blurring and significant loss of

details during the denoising process due to uneven illumination and complex environmental conditions. Gaussian filtering fails to preserve the track edges effectively. The classical BM3D algorithm greatly improves the image quality but may result in excessive noise removal.

Considering the results in Fig.3 and Fig.4, the improved BM3D filtering algorithm shows significant

improvements in PSNR and SSIM metrics. It effectively eliminates noise in complex environments while preserving the edge information of the railway tracks and removing interference information connected to the tracks. Furthermore, it preserves the original information to a large extent, thereby enhancing the denoising effect in complex environments.

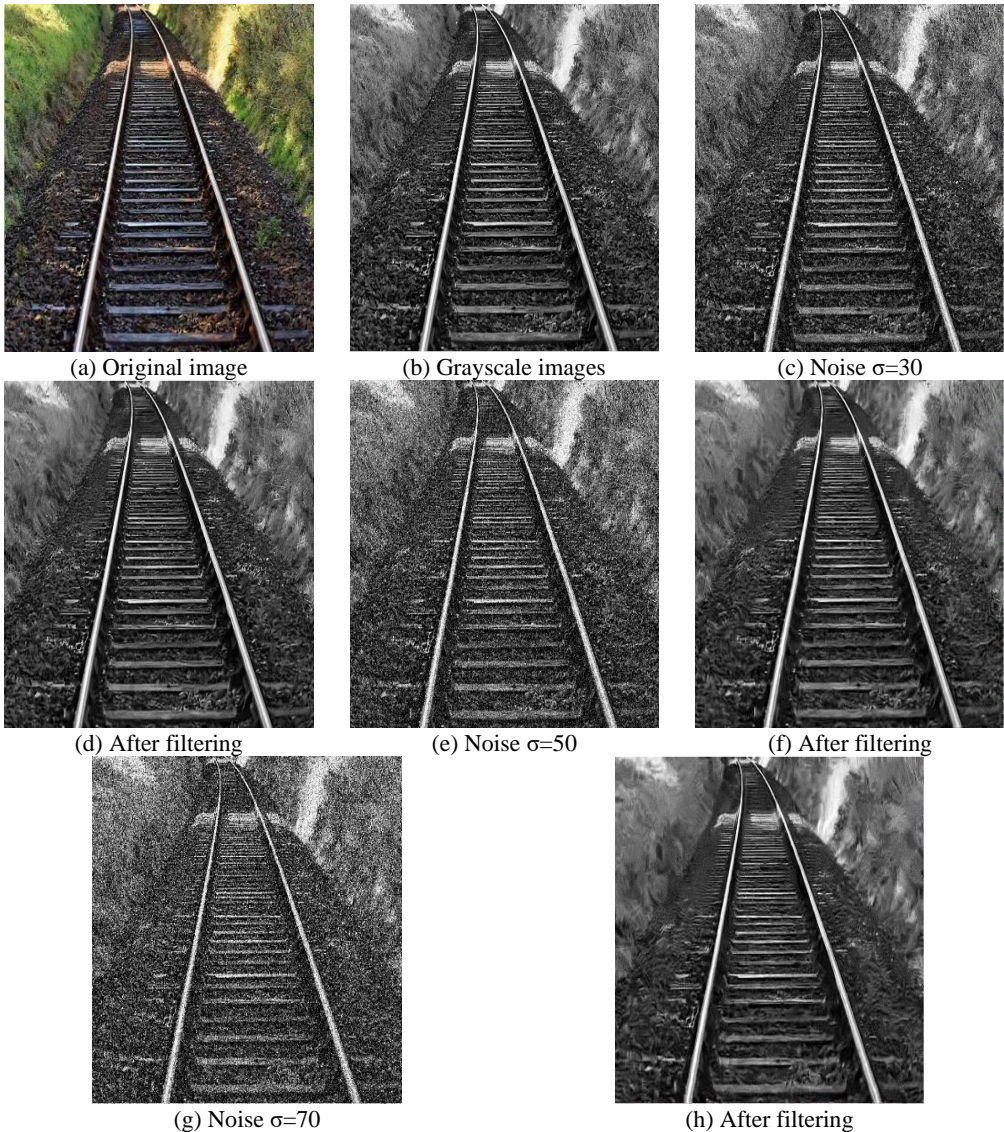


Fig. 2. Comparison image of the effect of different noise images after filtering

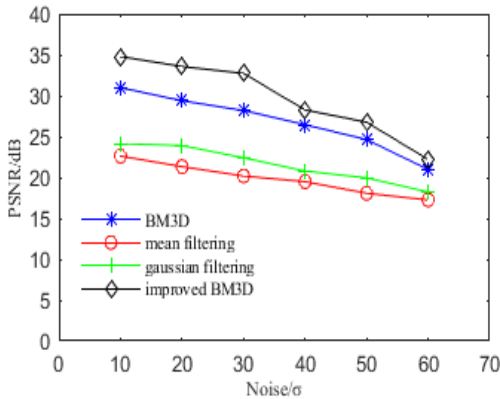


Fig. 3. Comparison chart of PSNR metrics of different algorithms

The results demonstrate the effectiveness of the improved filtering algorithm in reducing noise and preserving the important features of the railway tracks. The filtered images exhibit clearer track edges and a significant reduction in noise artifacts. This indicates that the proposed algorithm successfully enhances the quality of the images by effectively suppressing the noise while preserving the track details. The experimental results validate the feasibility and efficacy of the proposed improved filtering algorithm for railway track images.

5.2. Edge detection algorithm experiment

To validate the edge detection performance of the algorithm, we conducted experiments using railway images from different scenarios. For the railway tracks in scenario A and scenario B, we applied the original Canny algorithm, the algorithm mentioned proposed by Song et al. (2018), the algorithm mentioned proposed by Zhang et al. (2022), and the proposed algorithm in this paper for edge detection. A comparative analysis was performed on the detection results obtained from different algorithms.

By comparing the results in Fig.6 and Fig.7, we can analyze the effectiveness of different algorithms in extracting railway track edges. It can be observed that the original Canny algorithm lacks sufficient filtering capability, resulting in a significant amount of noise and overlap between distant interference and the railway track edges. The algorithm one has deficiencies in filtering and is susceptible to illumination shadows, leading to the presence of false edges. Due

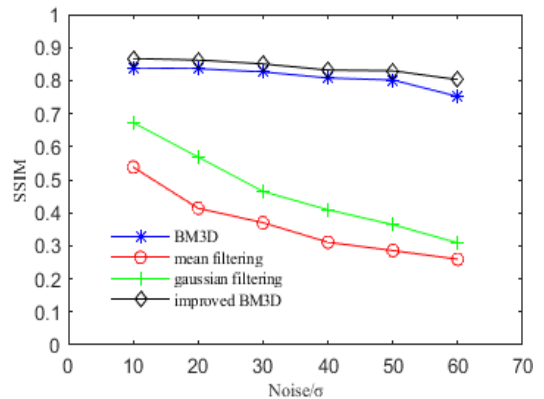


Fig. 4. Comparison chart of SSIM metrics of different algorithms

to the influence of shadows in the surrounding environment, the algorithm two cannot accurately detect the track edges, resulting in discontinuous detection. While all these algorithms preserve the characteristics of the railway track edges, they also retain image noise and some interfering information. Based on a comprehensive comparative analysis, we can conclude that the proposed algorithm in this paper effectively extracts the complete linear characteristics in the track images, preserves the edge information of the railway tracks, and efficiently removes noise and redundant interference from the environment. As a result, it achieves clear and continuous track edge detection results.

To objectively evaluate the edge extraction performance of the proposed algorithm, we used the Image Edge Definition (IED) statistical criterion (Tang et al., 2021) for quantitative analysis. The IED index is calculated as follows:

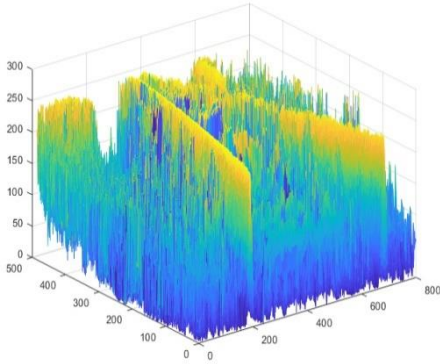
$$I=10 \left| \frac{\lg(\sum_{i=2}^{N-1} \sum_{j=2}^{M-1} N^2(i, j))}{(N-2)(M-2)} \right| \quad (23)$$

where $N(i, j)$ denotes the pixel value size of the edge image at (i, j) ; M and N denote the length and width of the edge image pixels. The IED values of different algorithms are shown in Table 1.

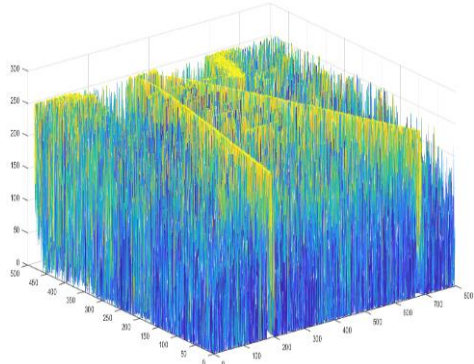
Based on Table 1, it can be observed that the classical Canny algorithm has lower edge clarity and longer detection time due to the influence of the background region. The algorithm one achieves higher image clarity and reduces the detection time to some extent. However, the algorithm two has

lower detection clarity in scenario B compared to the classical Canny algorithm. On the other hand, the proposed algorithm in this paper detects railway

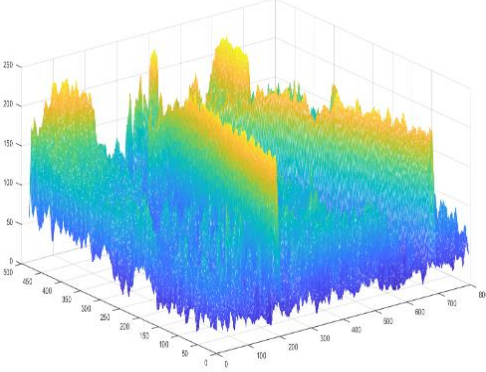
edge images with higher IED values and improves the edge detection time.



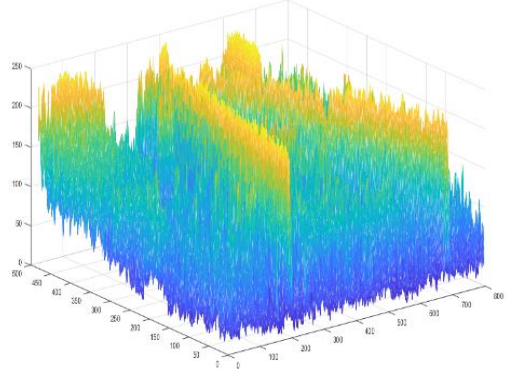
(a) 3D histogram of the original image



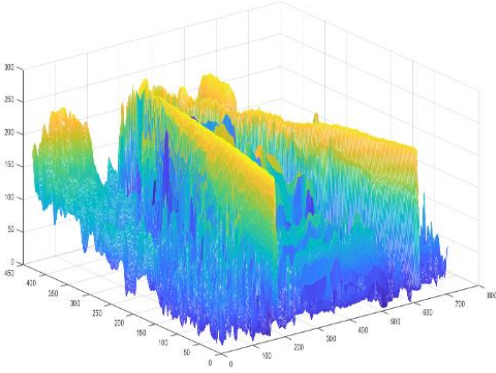
(b) 3D histogram of noise-added images



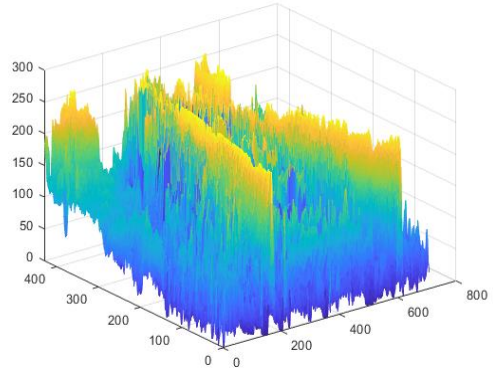
(c) Mean filtering



(d) Gaussian filtering



(e) BM3D



(f) Improved BM3D

Fig. 5. Comparison of 3D histograms after processing by different algorithm

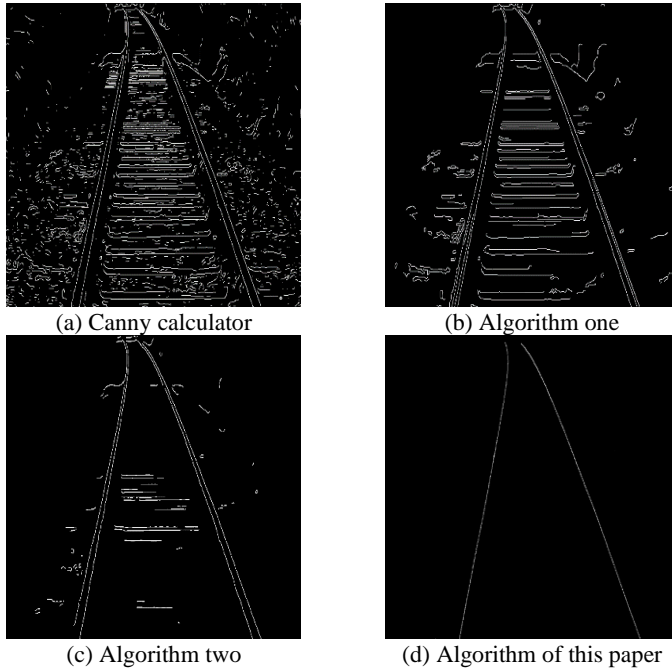


Fig. 6. Scene A Results of track edge detection by different algorithms

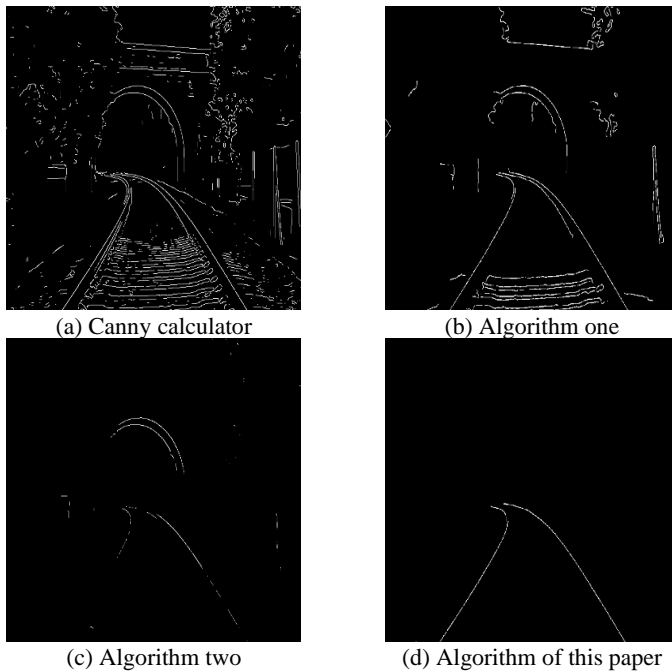


Fig. 7. Scene B Results of track edge detection by different algorithms

Table 1. Comparison of IED values and detection time after detection of track images of scene A and scene B

Methods	IED values for scene A	Detection time of scene A (s)	IED values for scene B	Detection time of scene B (s)
The classical Canny algorithm	18.671	0.582	17.061	0.602
Algorithm one	19.246	0.483	19.398	0.524
Algorithm two	18.9347	0.544	16.753	0.557
Algorithm of this paper	24.2892	0.457	22.742	0.468

Experimental results demonstrate that the proposed algorithm effectively filters out interference information in railway images, overcoming issues such as discontinuity and significant errors that often occur during edge detection. It successfully extracts railway track edges while preserving their long and continuous characteristics. Visual analysis of the edge detection results reveals that the enhanced Canny algorithm captures the details of railway track edges and provides clear and continuous edge information. The algorithm demonstrates robustness in handling variations in lighting conditions and complex background environments, enhancing the overall edge detection process. Compared to other algorithms, the proposed algorithm exhibits remarkable accuracy and robustness in edge detection. It shows improved performance in handling complex backgrounds and varying lighting conditions. The algorithm effectively suppresses noise and erroneous edges, resulting in more accurate edge detection results. Furthermore, it demonstrates the ability to adapt to different track orientations, making it suitable for various railway image scenarios. The algorithm successfully detects railway track edges in both scenario A and scenario B, providing clear and continuous edge information. It retains the characteristics of track edges, improves the connectivity of edges, and enhances the efficiency of railway edge detection.

In conclusion, the experimental results and analysis validate that the proposed edge detection algorithm outperforms other tested algorithms in terms of railway edge detection. Its effectiveness in handling interference, achieving continuity and accuracy in extracting railway track edges, is confirmed. The algorithm demonstrates excellent performance in terms of robustness, accuracy, and adaptability, providing reliable and accurate edge information for further analysis and applications.

6. Conclusions

This study focuses on the issues present in the existing railway track edge detection and conducts research on railway track edge detection based on improved BM3D and Zernike moments. By applying the improved BM3D filtering algorithm to the railway track images, we effectively eliminate interference from complex environments while successfully preserving the edge features of the tracks. In terms of global pixel-level edge detection, we have improved the original Canny algorithm by incorporating additional gradient calculation directions, increasing the computation template, and integrating the Otsu threshold segmentation algorithm, resulting in edge detection results with enhanced details. Additionally, in the local sub-pixel level edge detection, we propose a method based on Zernike moments to calculate the sub-pixel edges near the track edges, effectively reducing the computational load during the edge detection process.

Experimental verification demonstrates the outstanding performance of our algorithm in railway track edge detection. Compared to other algorithms, our approach significantly reduces the occurrence of false edges and shortens the detection time. Most importantly, our algorithm provides clear and continuous detection results of track edges, preserving the edge features of the railway track images effectively. The experimental results show that our algorithm successfully eliminates interference and noise while extracting complete linear characteristics, providing a reliable foundation for subsequent track detection and analysis.

However, we acknowledge that this study still has certain limitations. For instance, the algorithm may face challenges when dealing with specific lighting conditions or complex backgrounds. Therefore, future research can explore additional image feature

extraction methods or the application of deep learning techniques to further enhance the performance and robustness of railway track edge detection.

In conclusion, the improved algorithm presented in this study has achieved significant advancements in railway track edge detection. By enhancing the accuracy of edge detection, eliminating interference, and preserving edge features, we provide a reliable and effective method for the safety monitoring and maintenance of railway tracks. This research offers valuable insights and references for further research and application in the field of railway track edge detection.

Acknowledgements

This work was supported by Natural Science Foundation of Gansu Province(Grant No. 21JR7RA321, Grant No. 22JR5RA358).

References

- [1] Archana, P., Karunakar, B., (2019). Image segmentation using improved Canny algorithm and mathematical morphology. *Journal of Innovation in Electronics and Communication Engineering*, 8(2), 48-53.
- [2] Burdzik, R., Nowak, B., Rozmus, J., Pawe Sowiński, Pankiewicz, J., (2017). Safety in the railway industry. *Archives of Transport*, 44(4), 15-24.
<https://doi.org/10.5604/01.3001.0010.6158>
- [3] Cui, C. C., Zhou, X. C., Zan, M. Y., (2021). Image BM3D denoising method based on applying adaptive filtering. *Electronic Measurement Technology*, 44(12), 97-101.
- [4] Fu, J. H., Wang, J. P., Wen, L. H., et al. (2020). Bright-field stem cell image segmentation based on improved threshold and edge gradient. *Electronic Measurement Technology*, 43(20), 109-114.
- [5] Gong, S., Li, G., Zhang, Y., Li, C., Yu, L., (2019). Application of static gesture segmentation based on an improved canny operator. *The Journal of Engineering*, 2019(15), 543-546.
<https://doi.org/10.1049/joe.2018.9377>
- [6] Goyal, B., Dogra, A., Sharma, A. M., (2020). BM3D outperforms major benchmarks in denoising: an argument in favor. *Journal of Computer Science*, 16(6), 838-847.
<https://doi.org/10.3844/jcssp.2020.838.847>
- [7] Karolak, J., (2021). Interface and connection model in the railway traffic control system. *Archives of Transport*, 58(2), 137-147.
<https://doi.org/10.5604/01.3001.0014.9086>
- [8] Liu, H. Z., Ning, J., Zou, Q. H., et al. (2022). Research on feature extraction technology of Mineral zoning image of spiral concentrator based on deep learning. *Nonferrous Metals Engineering*, 12(12), 91-99.
- [9] Liu, J., Zhao, J. Y., Chi, Y., (2021). Subpixel detection of weld center line based on Zernike moment algorithm. *Journal of Shenyang Ligong University*, 040(004), 1-5+10.
- [10] Liu, K., Li, L., Tan, F., (2020). A Design of Intelligent Foreign Object Intrusion Detection System in Subway Station Track Area. International conference on transportation engineering.
<https://doi.org/10.1061/9780784482742.126>
- [11] Liu, Y., Cheng, M. M., Hu, X. W., Bai, X. et al. (2019). Richer convolutional features for edge detection. *IEEE transactions on pattern analysis and machine intelligence*, 41(8), 1939-1946.
<https://doi.org/10.1109/TPAMI.2018.2878849>
- [12] Luo, W. T., Li, Z. Y., Li, L., et al. (2018). Automated lane marking identification based on improved canny edge detection algorithm. *Journal of Southwest Jiaotong University*, 53(06), 1253-1260.
- [13] Lv, H., Shan, P., Shi, H., Zhao, L., (2022). An adaptive bilateral filtering method based on improved convolution kernel used for infrared image enhancement. *Signal, Image and Video Processing*, 16(8), 2231-2237.
<https://doi.org/10.1007/s11760-022-02188-1>
- [14] Niu, H. X., Hou, T., (2018). Fast detection study of foreign object intrusion on railway track. *Archives of Transport*, 47(3), 79-89.
<https://doi.org/10.5604/01.3001.0012.6510>
- [15] Ou, Y., Luo, J. Q., Xiong, Y., et al. (2020). Rivet size detection based on adaptive threshold Zernike moment. *Transducer and Microsystem Technologies*, 39(03), 139-142+152.
- [16] Polak, K., Korzeb, J., (2022). Modelling the acoustic signature and noise propagation of high speed railway vehicle. *Archives of Transport*, 64(4), 73-87.
<https://doi.org/10.5604/01.3001.0016.1051>

- [17] Ren, K. Q., Zhang, J. R., (2018). Extraction of plant leaf vein edges based on fuzzy enhancement and improved Canny. *Journal of Optoelectronics&Laser*, 29(11), 1251-1258.
- [18] Rosnelly, R., (2020). Combination of thresholding and Otsu method in increasing results of identification of malaria parasite type in thin blood smear image. *International Journal of Psychosocial Rehabilitation*, 24(4), 3807-3818. <https://doi.org/10.37200/IJPR/V24I4/PR201494>
- [19] Sheshathri, V., Sukumaran, S., Manju, M., (2019). Improved Canny edge detection method for affected leaves. *International Journal of Advanced Science and Technology*, 28(17), 877-885.
- [20] Soilán, M., Nóvoa, A., Sánchez-Rodríguez, A., et al. (2021). Fully Automated Methodology for the Delineation of Railway Lanes and the Generation of IFC Alignment Models Using 3D Point Cloud Data. *Automation in Construction*, 126,103684. <https://doi.org/10.1016/j.autcon.2021.103684>
- [21] Song, R. J., Liu, C., Wang, B. J., (2018). Adaptive Canny edge detection algorithm. *Journal of Nanjing University of Posts and Telecommunications (Natural Science Edition)*, 38(03), 72-76.
- [22] Song, Y. F., Pan, D. F., Han, H., (2018). Track detection approach in complex environment based on saliency features. *Journal of Railway Science and Engineering*, 15(04), 871-879.
- [23] Tang, M. A., Wang, C. Y., (2021). Extraction of the edge of track images based on improved canny algorithm and hough transform. *Railway Standard Design*, 65(8), 60-64.
- [24] Wang, B., Wang, Z., Zhao, D., Wang, X. H., (2022). A rail detection algorithm for accurate recognition of train fuzzy video. *Cyber-Physical Systems*, 8(1), 67-84. <https://doi.org/10.1080/23335777.2021.1879277>
- [25] Wang, Z. L., Cai, B. G., (2017). Geometry constraints-based method for visual rail track extraction. *Journal of Transportation Systems Engineering and Information Technology*, 17(06), 56-62, 84.
- [26] Wei, C. T., Yu, J. C., Zhao, P., et al. (2019). Automatic detection method of small cracks and micro grayscale difference cracks based on adaptive threshold. *Journal of China and Foreign Highway*, 39(01), 58-63.
- [27] Zhang, J. C., Xu X. G., Ye J., (2022). Image edge detection method based on improved Canny operator. *Journal of Hainan Tropical Ocean University*, 29(05), 79-84.
- [28] Zhang, J. C., Xu, X. G., Ye, J., (2022). Image edge detection method based on improved Canny operator. *Journal of Hainan Tropical Ocean University*, 29(05), 79-84.
- [29] Zhang, Y. (2022). Research on rail identification based 3D point cloud. Qinhuangdao: Yanshan University.
- [30] Zheng, J. F., Gao, Y. C., Zhang, H., Lei, Y. Zhang, J., (2022). OTSU Multi-Threshold Image Segmentation Based on Improved Particle Swarm Algorithm. *Applied Sciences*. 12(22), 11514-11514. <https://doi.org/10.3390/app122211514>
- [31] Zheng, Y. S., Yan, W. J., Yu, D., (2020). Rail detection based on LSD and the least square curve fitting. *International Journal of Automation and Computing*, 18(1), 1-11. <https://doi.org/10.1007/s11633-020-1241-4>